Astronomy & Astrophysics manuscript no. yzcnc-resubmitted March 9, 2004
(DOI: will be inserted by hand later)

XMM-Newton observations of the dwarf nova YZ Cnc in quiescence

Pasi Hakala[1], Gavin Ramsay[2], Peter Wheatley[3], Emilios Harlaftis[4], and C. Papadimitriou[5]

[1]Observatory, P.O. Box 14, FIN-00014 University of Helsinki, Finland
[2]Mullard Space Science Lab, University College London, Holmbury St. Mary, Dorking, Surrey, RH5 6NT, UK
[3]Department of Physics & Astronomy, University of Leicester, University Road, Leicester, LE1 7RH, UK
[4]Institute of Space Applications and Remote Sensing, National Observatory of Athens, P.O. Box 20048, Athens - 11810, Greece
[5]Institute of Astronomy & Astrophysics, National Observatory of Athens, P.O. Box 20048, Greece.

Abstract.
We present results from the *XMM-Newton* observations of the dwarf nova YZ Cnc in a quiescent state. We have performed a detailed time series analysis of the resulting light curves. Unusually, we do not detect any orbital modulation in the UV, with only marginal evidence for X-ray modulation on this period. Although there are peaks in the X-ray periodograms at periods less than 5000 s, we attribute them to red noise effects and assign significance to them using a novel approach. The variability in the UV and optical bands can also be modelled as a result of aperiodic variability (red noise) in the system. There is evidence that the UV and X-ray fluxes are anti-correlated with a time delay of about 100 s, with the UV lagging behind the X-ray emission. This anti-correlation is intriguing, but is only present on two occasions lasting several 1000 s each. The X-ray spectrum shows similar emission features to other dwarf novae and is well fitted using a multi-temperature emission model. We measure a relatively high X-ray luminosity of $\sim 1.4 \times 10^{32}$ ergs/s, although this is consistent with a low binary inclination. Finally, we find evidence for a possible -1200km/s blue shift in the fitted Fe K line energies, possibly indicating the presence of an outflow in this low inclination system.

Key words. accretion, accretion discs – stars: individual: YZ Cnc – novae, cataclysmic variables – X-rays: stars

1. Introduction

Dwarf novae are interacting stellar binary systems in which material gets transfered from a red dwarf secondary star onto a white dwarf via Roche lobe overflow. In the absence of a strong magnetic field this material forms an accretion disk around the white dwarf. They show outbursts which occur on week to month timescales. They have been well studied in many energy bands, including the optical and X-ray bands. In X-rays, the emission is suppressed during an outburst while it only recovers at the end of the optical outburst (eg Wheatley et al 1996). This is due to the gas being optically thick during outburst but optically thin in quiescence (eg Popham & Narayan 1995).

YZ Cnc is a dwarf nova with an orbital period of 125.17 min (van Paradijs et al 1994). It is also a member of the SU UMa class of dwarf novae - systems which show normal dwarf novae outbursts and also longer and brighter outbursts. UV observations show strong lines with P Cygni profiles which vary in shape over the orbital period - this was interpreted as an asymmetry in the wind flow pattern (Drew & Verbunt 1988, Woods et al 1992). White light observations by Pezzuto, Bernacca & Stagni (1992) show some evidence for dwarf nova oscillations on a period of 26 s, although this was only seen on one night.

The most prominent period seen in dwarf novae in the optical band is the binary orbital period. Other observed periods include the superhump period (which is due to disc precession), dwarf novae oscillations (on timescales of several 10's of s) and quasi-periodic oscillations which have also been seen in X-rays and have modulation periods of ∼100-1000 s (eg Patterson, Robinson & Nather 1977, Woudt & Warner 2002 and references therein).

Unlike the magnetic systems, direct evidence of the spin period of the white dwarf has been hard to come by. Recently, observations using *XMM-Newton* of the dwarf nova OY Car showed the X-rays varied on a timescale of 2240 s (Ramsay et al 2001a): the amplitude of this variation was stronger at soft X-rays. A further investigation also showed a period near 3500 s (Hakala & Ramsay 2003). They interpreted the 2240 s period as the spin period of

Send offprint requests to: P. Hakala

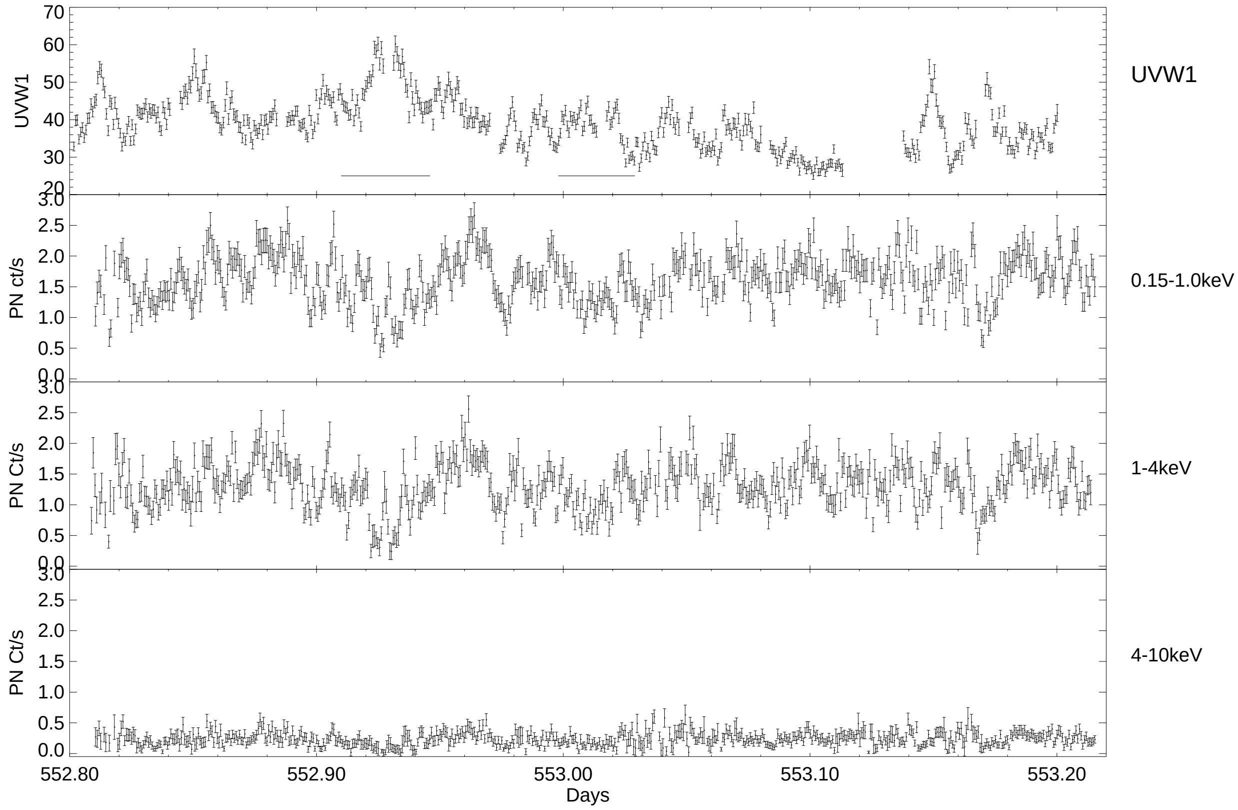

Fig. 1. The light curves of YZ Cnc, from the top; the UV data; 0.15-1.0keV, 1–4keV and 4–10keV. The date is HJD-2452000.0. The bin size is 60 s. The times of anti-correlation between the X-ray and UV bands are shown with horizontal lines in the top panel.

the white dwarf and the 3500 s period as a beat between the spin and the binary orbital period.

This led us to investigate whether other dwarf novae, if they are observed for a sufficiently long time, and with X-ray detectors of sufficiently large area, show similar evidence for variations which could be attributed to the spin period of the white dwarf. We have obtained observations of YZ Cnc using *XMM-Newton* which cover ∼4.5 orbital cycles. Our prime goal was to search for modulations in the X-ray and UV light curves. Here we present the results of our time series analysis. We also model the X-ray spectra and compare it with previous X-ray observations of dwarf novae.

2. Observations

2.1. XMM-Newton observations

XMM-Newton was launched in Dec 1999 and has the largest effective area of any imaging X-ray telescope. It has 3 medium spectral resolution CCD type cameras onboard: two EPIC MOS detectors (Turner et al 2001) and one EPIC pn detector (Stüder et al 2001). In addition it has two high resolution grating spectrographs (RGS), den Herder et al (2001). Further, it has an 0.3m optical/UV imaging telescope (the OM) which enables simultaneous X-ray optical/UV observations (Mason et al 2001).

YZ Cnc was observed using *XMM-Newton* during 5 Oct 2002: the observation log is shown in Table 1. The OM was configured in fast mode and used the UVW1 filter which has an effective wavelength of 2910Å(range 2400–3200Å). The data were processed using the *XMM-Newton* Science Analysis System v5.4. Data were extracted from an aperture centered on YZ Cnc and also from source free areas of the detector and suitably scaled to produce background subtracted light curves and spectra. Events times were corrected to the arrival at the solar system barycenter. For lightcurves, events with PATTERN=0-12 were used, while for spectra we used PATTERN=0-4. We only used events with FLAG=0 (See for instance XMM-User Guide or XMM- ABC guide (heasarc.gsfc.nasa.gov/docs/xmm/abc/) for discussion on different flags on data). Various (short) time intervals were removed during the standard processing because of high particle background events. We have analysed the observations made using both the EPIC pn and EPIC MOS detectors. For brevity, in the timing study we report only the EPIC pn data (the EPIC MOS data is consistent with the results found from the EPIC pn data), while in the spectral analysis we utilise all the X-ray data. The EPIC pn and OM light curves covering the whole observation are shown in Figure 1.

We can compare our observed count rate (3.4 ct/s in the 0.15-10keV EPIC pn energy band) with that seen using *Rosat*, when it was observed in outburst and quiesence (Verbunt, Wheatley & Mattei 1999). We assumed a thermal plasma model and relatively low absorption

EPIC pn	full-frame	thin	35506
EPIC MOS	full-frame	thin	36837
EPIC RGS	full-frame	thin	36977
OM	fast	UVW1	29700
Optical	V	2002-10-09	1hr 50min

Table 1. The observation log for XMM-Newton observations of YZ Cnc

($N_H = 1\times10^{20}$ cm^{-2}). Based on the counts observed using *ROSAT*, and using `PIMMS`, we expect 0.8 ct/s and 3.6 ct/s in the EPIC pn for YZ Cnc in outburst and quiescence respectively. Our *XMM-Newton* X-ray observations indicate that YZ Cnc was in a quiesence state at the time of observation. This is also confirmed from the optical AAVSO data.

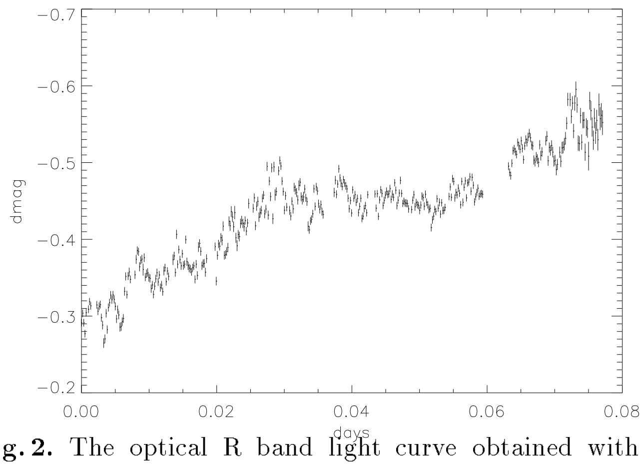

Fig. 2. The optical R band light curve obtained with a 1.2m telescope of Kryoneri station of the National Observatory of Athens covering 89% of the orbital period.

2.2. Ground based optical observations

Observations obtained from the AAVSO show YZ Cnc was in outburst ∼2 weeks before the *XMM-Newton* observations. A CCD V band AAVSO observation taken on the day of the *XMM-Newton* observations show YZ Cnc was at 15.2 mag - consistent with YZ Cnc being in quiescence.

R-band (Bessell filter) data with a time resolution of 12 s were obtained on 9 Oct 2002 (4 days after the *XMM-Newton* observations) with the 1.2m telescope at the Kryoneri station of the National Observatory of Athens. In total, 390 CCD images - covering 0.9 of the binary orbit were obtained. A comparison star was included in the field of view so that differential photometry could be obtained. The images were reduced in the standard manner. The resulting light curve is shown in Figure 2.

Further AAVSO observations show that YZ Cnc started to brighten 1–2 days after the *XMM-Newton* observations and reached V=12.2 on the day of our R-band observations. The R-band observations were therefore taken when the system was brightening to outburst. The rise is probably also evident in our optical data (Figure 2) , even if it is not possible to properly separate the rising trend from the orbital modulation due to the limited time baseline.

3. Light Curve analysis

We show the unfolded light curves in Figure 1. The UV data shows prominent flaring activity, with the 'flares' lasting several 100 s. There appears to be modulation on shorter periods as well. Variability is evident in all X-ray energy bands, and it is more pronounced in the first half of the observation.

3.1. Power Spectra

To make a more detailed investigation of the time variability we obtained a light curve in the 0.2-4keV energy band. We used the standard Lomb-Scargle power spectrum analysis. We show the resulting power spectrum in Figure 3 (together with significance limits). The most prominent peak is at 0.11 days (9300 s). A second broad feature is seen at 7000 s. These peaks are rather wide due to the 35 ksec length of the observation. Thus they are consistent with them being due to the orbital modulation and a beat period between the orbital modulation and the observation window length. However, we also analysed the light curves in two equal parts and this analysis showed that these broad spikes are only present in the first half of the data: this is clear from Figure 1, where most of the longer term X-ray variability seems to disappear towards the end of the run. There are also several spikes at shorter periods, which based on this initial analysis appear significant, but the confidence limits derived in Sect 3.2 and plotted in Figure 3 show that these peaks are not significant.

We also performed a similar analysis on the UV and optical data using the Lomb-Scargle method. The UV data did not show any evidence for the orbital period so only an analysis of shorter periods is presented here. The optical data only covers 0.9 of the orbital period, so again only short period analysis is presented.

We show in Figure 4 the power spectra in the optical and UV covering the period range up to 3000 s. The strongest spike in the UV periodogram (top panel) is the spike near 1530 s. From our red noise analysis, we can however conclude that this spike is less than 99% significant. A spike near at a similar period is seen in the R band (lower panel). The fact that the R band spike is much wider is due to the short length of the optical observations. The R band power spectrum also shows another, stronger spike at about 800 s. This spike is, within the error limits, the second harmonic term of the 1530 s period and could possibly appear in the power spectrum due to a double peaked nature of the optical modulation. However, also none of the R band spikes exceed the 99.9% threshold obtained from the red noise analysis.

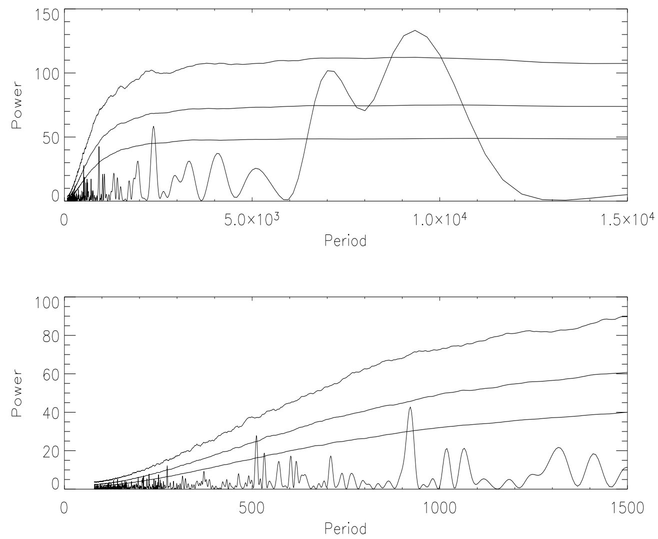

Fig. 3. The power spectrum of the 0.2–4keV EPIC pn light curve. 90%, 99% and 99.9% confidence limits from the Monte Carlo simulations (including white and fitted red noise) are shown with horizontal lines. The lower panel is a blowup of the upper panel at shorter periods.

3.2. Red Noise effects

It is well known that a presence of red noise (noise dominated by low frequencies) in the data can lead to appearance of spurious spikes in the power spectra. This 'noise' is produced by low frequency aperiodic (random walk type) intrinsic variability in the source (i.e. flickering). In order to obtain confidence limits which take into account these effects in the power spectrum analysis, we have proceeded to model the X-ray and UV data with time series analysis tools commonly used in analyzing evenly sampled time series data in other fields (see for instance Chatfield, 1989) . The autoregressive processes used here have also previously been used in context of astronomical data analysis (see for instance Roques, Schwarzenberg-Czerny, Dolez, 2000 and Chen et al. 2000), but not, in our knowledge, for estimating the significance of peaks in power spectrum in the presence of red noise.

In order to apply these techniques the data must be evenly spaced in time. As both X-ray and UV data contain short gaps, we need to interpolate flux values for these times (cf. §2). However, as these gaps are very short in time and only account for a very small fraction of the total light curve, we believe our approach is justified.

Our approach begins with modelling of the time series as an Autoregressive (AR) process, where the flux at time t, F_t depends on the fluxes at times $t-1, t-2, ..., t-n$ in the following manner:

$$F_t = \sum_{i=1}^{n} \alpha_i (F_{t-i} - \overline{F}) + Gauss(\overline{F}, F_\sigma) \qquad (1)$$

where $\overline{F}$ is the mean flux, F_σ is the standard deviation of the white noise component and $Gauss(\overline{F}, F_\sigma)$ is a Gaussian random variable with mean $\overline{F}$ and standard deviation F_σ). Depending on the choice of n we have AR processes of different order (AR(1), AR(2), ..., AR(n)).

Fitting an AR process to the time series is a straight forward linear least squares problem. Let $\mathbf{R}$ be the autocorrelation matrix of a given time series (up to the lag n-1), and $\mathbf{r}^T$ be a vector of autocorrelations: $\mathbf{r}^T = (r_1, r_2, ..., r_n)$. Then the α_i coefficients of the AR(n) process can be solved from the matrix equation:

$$\alpha = \mathbf{R^{-1}r} \qquad (2)$$

First tests, using X-ray data, with AR(1) and AR(2) model fits could not reproduce the original power law slope seen in the X-ray power spectrum. We then increased the AR process order to 7, which enabled us to reproduce the power spectrum slope correctly, thus indicating that the model then contained the right amount of red noise and other long period aperiodic variability. Actually the last (7th) coefficient α_7 was already an order of magnitude smaller than α_6 indicating that our AR(7) model contained enough orders. Figure 5. shows the X-ray power spectrum in log(f)-log(Power) space. Overplotted is our red noise fit using the AR(7) model, that clearly models the red noise in the data adequately.

Having reproduced the noise power spectrum satisfactorily, we then proceeded to create simulated data based on this model. This was done in the following manner: For every simulated data set we took the original time points and the AR(7) fit as the basis, but reshuffled the original data points and added them in random order to the values generated by the AR(7) process . The reason for using this bootstrap-like technique instead of pure gaussian random numbers is that at the observed count rate level, the flux distribution is Poissonian, not yet Gaussian. This process was repeated in order to produce 10000 simulated datasets, all of which contained all the long term aperiodic variability and red noise components, as well as the window and sampling effects present in the data. These "datasets" could then be used as a basis for reliable significance level estimates for the Lomb-Scargle power spectra. We have overplotted the resulting significance limits for X-ray data in Figure 3.

Similar analysis was performed on UV and optical data. For the UV observations, the data gaps were interpolated, but as the optical data was obtained during a continuous, evenly sampled observing run, no interpolation was required. Again, we generated 10000 fake light curves with similar (fitted) red noise properties as in the real data. Then the same Lomb-Scargle analysis was repeated for these fake datasets in order to produce the significance curves overplotted in Figure 4.

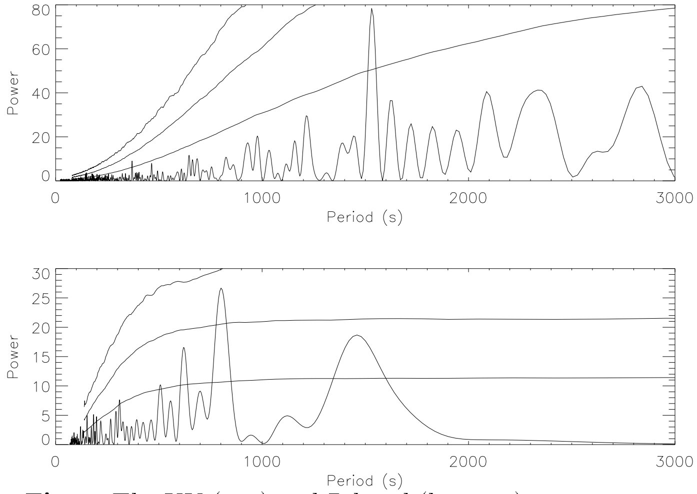

Fig. 4. The UV (top) and R band (bottom) power spectra with 90, 99 and 99.9% significance levels based on red noise fits.

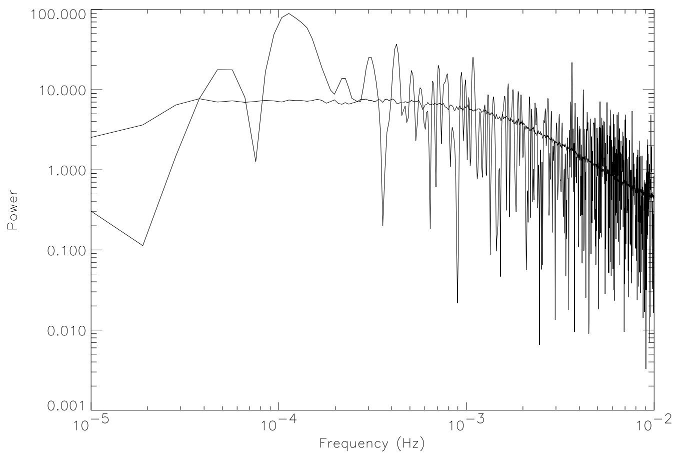

Fig. 5. The observed X-ray power spectrum continuum with an AR(7) red noise fit .

3.3. Significance of power spectra peaks

Our autoregression analysis is capable of explaining almost all spikes in the X-ray power spectrum as a result of red noise. The only exception is the 9300s spike, which however, as noted earlier, only appears in the first half of the data.

Similarly, even if clear spikes are seen in the optical and UV light curves, we can explain them as a result of intrinsic, aperiodic red noise type variability in the source. No spikes in UV or optical exceed the 99.9% (3.3σ) significance level. Furthemore the 1530s spike in the UV band is almost entirely dominated by the presence of two strong, flare like, events near the end of observation (at around 553.15-553.18, Figure 1.). If we only analyse the UV light curve before the large gap in data at around 553.12, the spike at 1530 s almost totally disappears from the power spectrum. This further strengthens the case for red noise interpretation.

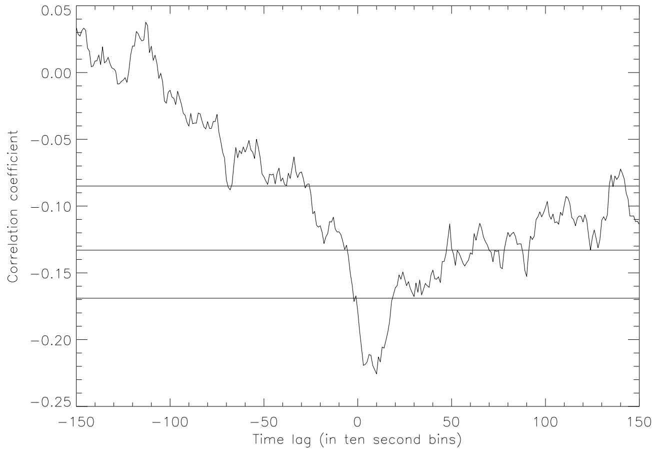

Fig. 6. The average cross correlation between the X-ray and UV bands. We have overplotted the 90%(top),99% and 99.9% significance limits from our Monte Carlo simulations.

4. The X-ray - UV cross correlation analysis

There is some suggestion from Figure 1 that there may be an anti-correlation between the UV and X-ray fluxes (for instance around 552.93 days). We have investigated this possibility using a cross-correlation analysis. Pandel, Cordova & Howell (2003) found that the X-ray and UV fluxes of VW Hyi are correlated with the X-ray flux following the UV with a 100 s time lag.

As the UV and X-ray time points are not exactly same, in order to compute the cross-correlation function the UV flux was interpolated to the X-ray time points. The time resolution used for the correlation analysis was 10 s. In addition to 'normal' cross-correlation analysis (Figure 6), we computed the cross-correlation function as a function of time using a sliding box that covered 10% of the observation length at the time. The resulting time dependent cross-correlation function is plotted in Figure 7. We find that, on average, timelags between –1500 to +1500 s show the UV and X-ray flux are more likely to be anti-correlated than correlated (Figure 6) . However, Figure 7 indicates that the average anti-correlation is dominated by two separate 'events' in the time series. During these events the cross-correlation function shows a clear minimum roughly at +100 s, which corresponds to the anti-correlated UV emission lagging 100 s behind the X-ray emission. The actual values for the correlation coefficients are however rather small. We discuss the physical implications of this in the Discussion section.

Attempting to estimate the significance of the possible anti-correlation with 100 s time lag, we have performed some Monte Carlo simulations. Using the fitted red noise models to the both X-ray and UV light curves we have then generated 30000 pairs of UV and X-ray light curves, that carry the same amount of red noise as the observed

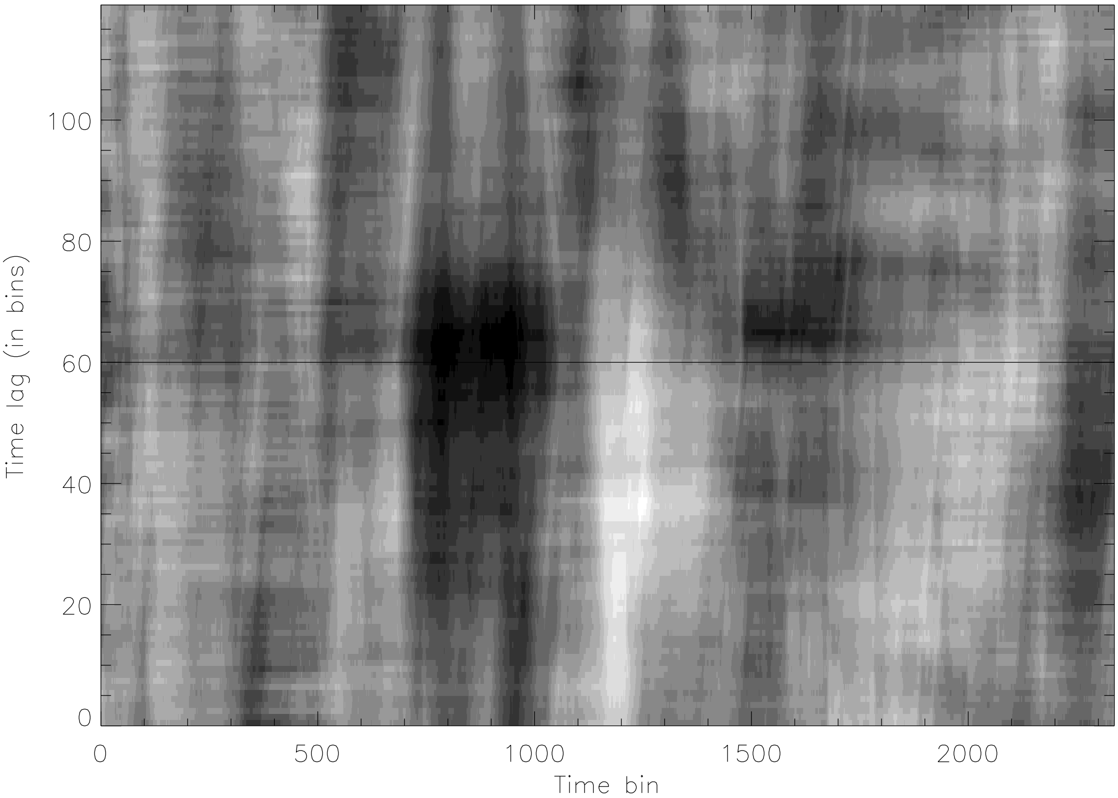

Fig. 7. The time dependent cross-correlation function between the X-ray and UV bands. The times of strong anticorrelation (darkest parts) are marked by horizontal lines in Figure 1.

data. We have then correlated them in order to estimate the distribution of correlation coefficients. From this exercise we find that only 3 out of 30000 correlations produce a correlation coefficient larger (in absolute value) than the value corresponding to the 100s delay (-0.225). The result was the same both for standard and rank correlation analysis. The resulting significance levels are overplotted in Figure 6.

However, we have to be cautious interpreting this result: Our simulations also show that the distribution of the correlation coefficients is sensitive to the amount of red noise in the data. Any underestimation of the amount of red noise in the data would lead to overestimation of the significance of the correlation.

5. X-ray spectra

5.1. EPIC spectra

We show the integrated EPIC pn spectrum in Figure 8: its shape is typical of a dwarf nova (eg Baskill, Wheatley & Osborne 2004). We fitted this spectrum with an absorbed (simple neutral absorber) single temperature thermal plasma model: this gave a poor fit (χ^2_ν=4.95 578dof). We then added a second and third plasma model, giving improved fits with χ^2_ν=1.87 (576dof) and χ^2_ν=1.47 (575dof) respectively. We then allowed the metal abundance to vary from solar, and obtained a fit of χ^2_ν=1.37 (573dof) with 1.5 solar abundance. We show the spectral parameters using this model in Table 2 and show the fit in Figure 8. There was a small improvement to the fit (better at the 99.4 per cent level, using an f-test, χ^2_ν=1.35, 571dof) when we added a neutral absorption model with partial covering component. We find a very similar fit when we fit the spectrum with a multi-temperature model with a power law distribution of emission measures (`cemekl` in `XSPEC`, χ^2_ν=1.37 574dof). This is similar to the results of *XMM-Newton* observations of the dwarf novae OY Car Ramsay et al (2001b) and VW Hyi (Pandel, Cordova & Howell 2003).

We also show the residuals to the fit in Figure 8: the residuals are prominent around the Fe Kα line. In particular the 6.7keV line appears at higher energies with respect to the model. We investigated this further by allowing the redshift to vary in the fit: we restricted the energy range to 5–8keV. With zero redshift we obtain a poor fit (χ^2_ν=2.31 63dof), while with a blue shift of 1200 km/s we get a significantly better fit (χ^2_ν=1.18 62dof). (The confidence interval at the 90 percent level is –1100 to –1500 km/s). Adding a Gaussian line at 6.4keV to model any fluoresent line (giving an equivalent width of 35eV, 16-53eV, 90% confidence limits) improves the fit even further (χ^2_ν=1.04 61dof). We show the spectrum together with this fit in

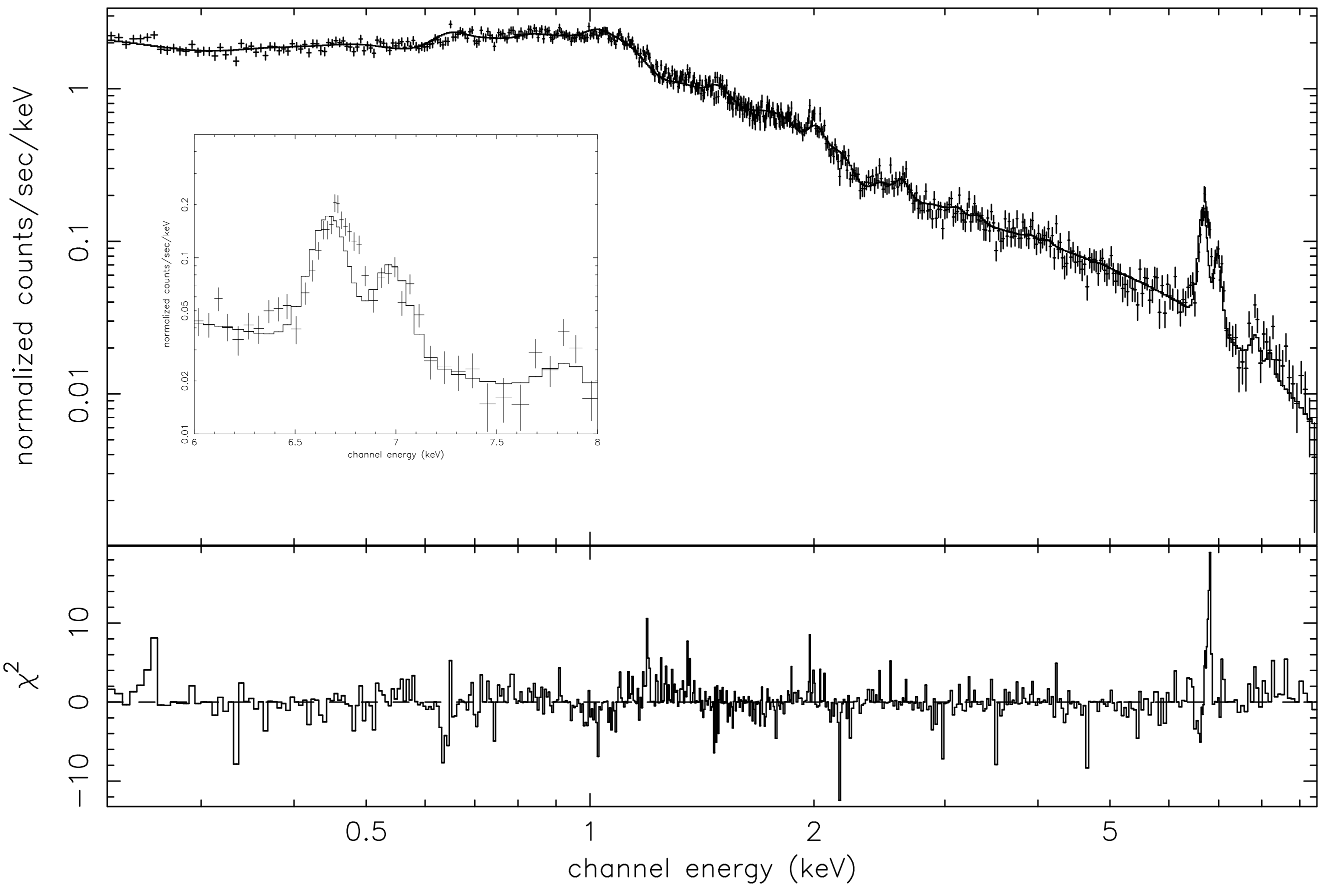

Fig. 8. The integrated EPIC pn spectrum of YZ Cnc together with a 3-temperature model fit.

Figure 9. We phased events on the orbital period and extracted four phase-resolved spectra: they all showed blue-shifts but, within their errors, showed no significant difference in their velocity shift.

We have considered the possibility that this blue-shift is not physical and due to instrument calibration effects. We have therefore examined the combined EPIC MOS data in the same manner as above. The best-fit blueshift is close to zero, with a 90 percent confidence interval of –630 to +340 km/s. The difference in the redshift for the 6.7keV line between the EPIC pn and MOS is therefore less than 2σ. Such 'instrumental blueshift effect' in EPIC pn data has not been previously reported (Frank Haberl, priv. comm.).

If we *do* attribute the blue-shift to a physical process, then the most likely cause is that we are viewing some kind of outflow, either wind from the disc or a jet. YZ Cnc has a relatively low inclination ($i \sim 30-35°$, Shafter & Hessman 1988): therefore higher inclination systems might be expected to show lower blue-shifts. We have re-examined the Fe Kα emission line complex of the eclipsing dwarf nova OY Car ($i = 83°$). We find that in the integrated EPIC pn spectrum the best fit red-shift is –220 km/s (the confidence interval at the 90 percent level is –780 to –170 km/s). This blue-shift is less than that determined in the EPIC pn observations of YZ Cnc. However, high signal-to-noise X-ray spectra of dwarf novae with a range of inclination angles is required to determine if this blue-shift can be attributed to a real physical affect.

N_H	$8^{+2}_{-0.2} \times 10^{19}$ cm^{-2}
kT (keV)	0.7±0.05, $2.0^{+0.1}_{-0.2}$, 8.3±0.5
Metal Abundance (solar)	1.5±0.1
Observed flux (0.2–10keV)	$9.24 \pm 0.4 \times 10^{-12}$ erg s^{-1} cm^{-2}
Bolometric flux	$1.21 \pm 0.05 \times 10^{-11}$ erg s^{-1} cm^{-2}

Table 2. The fits to the integrated EPIC pn spectra using a 3-temperature thermal plasma model with a neutral absorption model.

We note that there is evidence in the EPIC pn data for weak emission near 6.4keV which might be due to fluorescence from the photosphere of the white dwarf or cold material. Ramsay et al (2001b) suggested that its absence in OY Car was due to the high inclination of that system. In contrast, YZ Cnc is thought to have a relatively low inclination: this suggests that inclination does not have a strong influence on whether the 6.4keV line is detected. This is consistent with the findings of Baskill, Wheatley & Osborne (2004) who find that only 4 out of 34 dwarf novae showed a significant (equivalent width of up to 200eV) 6.4keV line in a survey using *ASCA*. Again there was no correlation with those systems which did show this line and their binary inclination. It is therefore unclear as to why some systems show this feature.

Thorstensen (2003) determines the distance to YZ Cnc to be 222^{+50}_{-42} pc from ground based parallax measurements, while Harrison et al (2003) determined a distance of 320±40 pc using HST FGS parallax observations. Thus the X-ray luminosity is likely to be about 1.4×10^{32} erg s^{-1}(assuming 300pc distance). At face value this is a rather high value for a quiescent dwarf nova. However, YZ Cnc has a relatively low inclination and the high X-ray luminosity is then consistent with van Teeseling, Beuermann & Verbunt (1996) who found that the observed flux is anti-correlated with inclination and thus in high inclination systems a significant fraction of the X-rays from the boundary layer are probably absorbed by the accretion disk. Furthermore, at least two systems (V603 Aql and SS Cyg) in Baskill et al. (2003) have luminosities similar or higher than YZ Cnc.

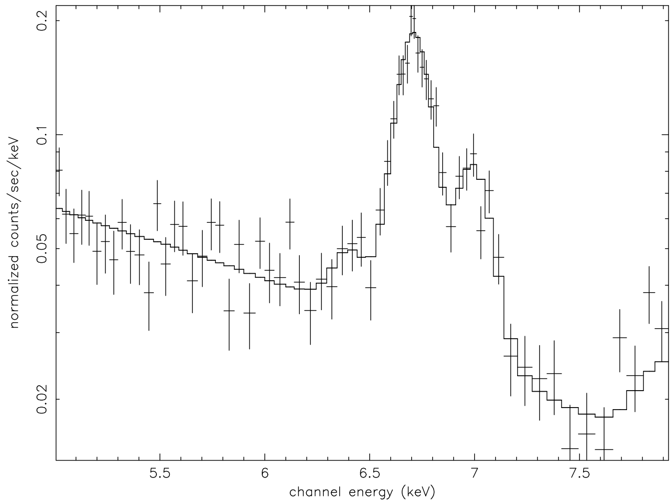

Fig. 9. The fit to the iron line complex with free radial velocity and a Gaussian profile at 6.4 keV added.

5.2. RGS spectra

We show the integrated RGS(1+2) spectrum in Figure 10. The most prominent feature is an emission line at 0.65keV which is due to OVIII Lymanα. Similar to VW Hyi (which also shows this prominent line), it is slightly broadend compared to the instrumental response (590 km/s, 120-770 km/s, 90% confidence). We show the spectrum compared with the best fit model obtained from the fits to EPIC pn spectrum. Although the signal to noise is relatively low there is evidence for other emission lines including Fe XVII (0.73keV), Fe XIX,XX (0.73keV), Fe XXI (1.02keV) and Fe XXIV (1.16keV). Such a range of charge states indicates a range of temperature regions, which is also implied by the need for multi-temperature spectral fits for the EPIC data.

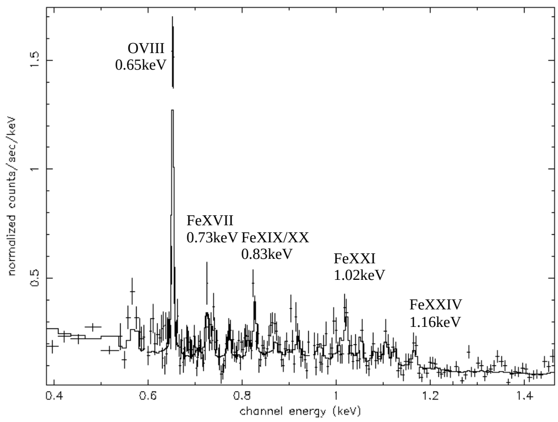

Fig. 10. The integrated RGS spectrum of YZ Cnc with the multi-temperature best model fit to the EPIC pn data shown as a solid line.

6. Discussion

The main aim of this programme was to obtain information about the temporal behaviour of YZ Cnc. In particular, the $XMM-Newton$ observations of a similar system OY Car (Ramsay et al. 2001a, Hakala & Ramsay, 2003) have indicated that the X-ray light curve could contain a significant white dwarf spin period component.

Our analysis of the EPIC and OM data has revealed intrinsic variability in the source, all of which can be attributed to the effects of red noise. Baskill et al. (2003), have analyzed a complete set of ASCA observations of non-magnetic CV's. They conclude that 7 out of 34 systems they have analyzed show evidence for X-ray modulation at the orbital period. Most of these systems, however, are high inclination systems in quiescent state. Thus the fact that we do not detect any persistent orbital modulation in our X-ray light curve is in agreement with the relatively low inclination of YZ Cnc.

According to our study, all the spikes seen in the X-ray power spectrum are due to the red noise. There is no sign for the previously reported 26s period that was earlier seen in the optical white light data during one single night (Pezzuto, Bernacca & Stagni, 1992) .

Curiously, also our OM UV data does not show any periodic modulation at all. Based on results of other dwarf novae (for instance OY Car, Ramsay et al., 2001a and VW Hyi, Pandel et al., 2003) an UV modulation due to the hot spot on the edge of the disc would be expected. However, recently Hakala & Ramsay (2003) showed using $XMM-Newton$ OM data that even in a high inclination system like OY Car, the hot spot modulation in quiescence is much more prominent in optical band than in UV. This, combined with the presumably low inclination, is the likely reason for nondetection.

Our cross-correlation analysis analysis has revealed that the X-ray and UV fluxes seem to be occasionally anti-correlated. This anti-correlation seems to be related to the times of UV flares as indicated in Figures 1 and 7. When the anti-correlation is present, the UV flares seems to lag behind the drop in X-ray emission by ~ 100 s. This is very curious: Lags at similar time scales have been observed in VW Hyi (Pandel et al. 2003), but in their case the X-rays and UV are correlated and the X-rays lag behind the UV. Such correlation arises naturally if the UV emission originates near the transition region from disc to the boundary layer and the propagation time of accretion rate fluctuations from the UV emitting region to the boundary layer (X-ray source) is of the order of 100s. Interestingly Pandel et al. (2003) also note that they see X-rays and UV vary strongly at time scales of 1500s, which also seems to be the case for UV emission in YZ Cnc.

Given that the variability time scale is the same, but the cross-correlation is opposite we have to conclude that the observed difference is most likely due to different viewing geometry (inclination) of the system. This is also suggested by the lack of orbital modulation in UV. However, the exact accretion geometry and/or physics that would produce such an effect as a function of inclination remains unresolved.

7. Conclusions

Our $XMM-Newton$ observations of YZ Cnc do not reveal any periodicities in the system, even if clear short term variability is present in both X-ray and UV bands. The cross-correlation analysis reveals that during major UV flares the X-rays and UV are anticorrelated, with UV lagging behind the X-rays by ~ 100 s. The measured X-ray luminosity, $\sim 1.4 \times 10^{32}$ erg s^{-1}, is relatively high for a dwarf nova in quiescent state. A multitemperature plasma model (possibly with a partially covering absorber) is required to model the X-ray spectrum. Finally we find that the iron line complex near 6.7 keV shows some evidence for blue shifted emission at about -1200 km/s. However, we cannot entirely rule out instrumental effects.

Acknowledgements. This paper is based on observations obtained with XMM-Newton, an ESA science mission with instruments and contributions directly funded by ESA Member States and the USA (NASA). PJH is an Academy of Finland research fellow. We acknowledge with thanks the variable star observations from the AAVSO International Database contributed by observers worldwide and used in this research.

References

Baskill, D., Wheatley, P., Osborne, J., 2003, MNRAS, submitted.
Chatfield, C., 1989, "The Analysis of Time Series, 4th ed.", Chapman and Hall Ltd, London.
Chen, L., Li, T.-P., Song, L.-M., Feng, Y.-X., 2000, Chinese Astronomy and Astrophysics, 24, 297.
Drew, J. E., Verbunt, F., 1988, MNRAS, 234, 341.
Hakala, P.J., Ramsay G., 2003, A&A, submitted.
Harrison, T. E., Howell, S. B., Huber, M. E., Osborne, H. L., Holtzman, J. A., Cash, J. L., &Gelino, D. M., 2003, AJ, 125, 2609.
den Herder, J.W., Brinkman, A.C., Kahn, S.M., et al. 2001, A&A, 365. L7.
Mason, K. O., et al, 2001, A&A, 365, L36
Pandel, D., Córdova, F., Howell, S., 2003, MNRAS, in press, (astroph/0309418).
Patterson, J., Robinson, E. L., Nather, R. E., 1977, ApJ, 214, 144.
van Paradijs, J., et al, 1994, MNRAS, 267, 465.
Pezzuto, S., Bernacca, P. L., Stagni, R., 1992, A&A, 257, 523.
Popham, R., Narayan, R., 1995, ApJ, 442, 337.
Ramsay, G., Poole, T., Mason, K., Córdova, F., Priedhorsky, W., Breeveld, A., Much, R., Osborne, J., Pandel, D., Potter, S., West, J., Wheatley, P., 2001a, A&A, 365, L288.
Ramsay, G., Córdova, F., Cottam, J., Mason, K., Much, R., Osborne, J., Pandel, D., Poole, T., Wheatley, P., 2001b, A&A, 365, L294.
Roques, S., Schwarzenberg-Czerny, A., Dolez, N., 2000, Baltic Astronomy, 9, 463.
Strüder, L., et al, 2001, A&A, 365, L18
van Teeseling, A., Beuermann, K., Verbunt, F., 1996, A&A, 315, 467
Thorstensen, J., 2003, AJ, in press, (astroph/0308516).
Turner, M.J.L., Abbey, A., Arnaud, M., et al. 2001, A&A, 365, L27.
Wheatley, P. J., Verbunt, F., Belloni, T., Watson, M. G., Naylor, T., Ishida, M., Duck, S. R., Pfeffermann, E., 1996, A&A, 307, 137.
Woods, J. A., Verbunt, F., Collier Cameron, A., Drew, J. E., Piters, A., 1992, MNRAS, 255, 237.
Woudt, P., Warner, B., 2002, MNRAS, 335, 44.